Master's Thesis

An organic-free electrolyte for stable lithium-oxygen batteries

Aming Cha

Department of Energy Engineering

(Battery Science and Technology)

Graduate School of UNIST

2018

An organic-free electrolyte for stable lithium-oxygen batteries

Aming Cha

Department of Energy Engineering
(Battery Science and Technology)

Graduate School of UNIST

An organic-free electrolyte for stable lithium-oxygen batteries

A thesis/dissertation
submitted to the Graduate School of UNIST
in partial fulfillment of the
requirements for the degree of
Master of Science

Aming Cha

1. 08. 2018
Approved by

_____

Advisor
Seok Ju Kang

An organic-free electrolyte for stable lithium-oxygen batteries

Aming Cha

This certifies that the thesis/dissertation of Aming Cha is approved.

1. 08. 2018

signature

_____

Advisor: Seok Ju Kang

signature

_____

Hyun-Kon Song

signature

_____

Nam-Soon Choi

Contents

Abstract

Aprotic electrolyte based lithium-oxygen batteries are of considerable interest due to its ultrahigh theoretical specific energy density (1675 mAh per gram of oxygen) against the present lithium-ion battery. In spite of the attractiveness of its high theoretical capacity, there is a number of drawbacks such as instability of electrochemical reaction of electrode and electrolytes. In order to overcome these parasitic reactions, significant efforts have been devoted to developing the key materials such as carbon-free air cathodes and high concentrated electrolytes. However, the CO_2 evolution during the charging process and low ionic conductivity limit the ideal electrochemical reaction in aprotic electrolytes.

In this thesis, we applied the molten electrolyte based on nitrate-based electrolyte (Li/Na/K/Cs/Ca-NO_3). The molten electrolyte, which has a eutectic point of 65℃, has the advantages of high stability and high-temperature operation, thereby preventing detrimental solvent byproducts in lithium-oxygen batteries. We examined the Oxygen Evolution Reaction (OER) and Oxygen Reduction Reaction (ORR) on operating temperature using in situ pressure drop and gas analyses, Differential Electrochemical Mass Spectrometry (DEMS). Our results demonstrated that the Li_2O_2, a discharge product, formed a stable hexagonal morphology in the lithium-oxygen battery upon discharge process by scanning electron microscopy and X-ray diffraction techniques. Also, it leads to improved oxygen mobility at high temperature since a molten salt was used as the electrolyte in lithium-oxygen batteries. In addition, we found that kinetics are improved with increasing operating temperature in molten salt electrolyte cells.

List of figures

Figure 2.4 Charge profile and gas evolution profile during charging of the cathode electrode pre-filled by Li_2CO_3 with Super P as conductive additive under argon atmosphere with Li foil as anode. (a.c) 1 M LiTFSI in TEGDME was used as organic electrolyte. (b,d) $LiNO_3$-KNO_3 molten salt was used as inorganic electrolyte.

Figure 2.5 Charge profile and gas evolution profile during charging of the cathode electrode pre-filled by Li_2CO_3 and Super P with Ir as catalyst for Li_2CO_3 decomposition under argon atmosphere with Li foil as anode. (a.c) 1 M LiTFSI in TEGDME was used as organic electrolyte. (b,d) $LiNO_3$-KNO_3 molten salt was used as inorganic electrolyte.

List of tables

Chapter 1

1. Organic-free electrolyte for stable lithium-oxygen batteries

1.1 Introduction of rechargeable lithium-oxygen batteries

Even though current developments of lithium-ion batteries have commercialized in the portable device market, there is a limit to meeting the needs of the electric vehicles (EV) market. For example, the current driving range of electric vehicles based on lithium-ion batteries is 200 km, which is not sufficient for long-distance driving.[1] On the other hand, the lithium-oxygen battery has an extremely high theoretical specific energy (3505 Wh kg^{-1}) as shown in Table 1 because it can store the discharge product, Li_2O_2 (lithium peroxide) in the pores of the cathode and uses light oxygen as a reactive product.[2-3]

Table 1. Characteristics for major electrochemical reactions of energy-storage devices.[2]

Battery	Cell Voltage (V)	Theoretical specific energy (Wh Kg^{-1})	Theoretical energy density (Wh l^{-1})
Today`s Li-ion $^1/_2C_6Li + Li_{0.5}CoO_2 \leftrightarrow 3C + LiCoO_2$	3.8	387	1,015
Zn-air $Zn + {}^1/_2O_2 \leftrightarrow ZnO$	1.65	1,086	6,091 (ZnO)
Li-S $2Li + S \leftrightarrow Li_2S$	2.2	2,567	2,199 ($Li + Li_2S$)
Li-O_2 (non-aqueous) **$2Li + O_2 \leftrightarrow Li_2O_2$**	**3.0**	**3,505**	**3,436 ($Li + Li_2O_2$)**
Li-O_2 (aqueous) $2Li + {}^1/_2O_2 + H_2O \leftrightarrow 2LiOH$	3.2	3,582	2,234 ($Li + H_2O + LiOH$)

The first lithium-oxygen battery was introduced in 1996 by Abraham and Jiang.[4] They used a polymer electrolyte membrane between the Li metal anode and the carbon electrode. A decade later, Bruce and his co-workers showed that the polymer electrolytes were replaced with organic electrolytes, resulting in a simpler structure and higher capacity than before. They has resulted in a worldwide contribution to the activation of lithium-oxygen battery research.[5] In addition, in 2012, Bruce *et al.* demonstrated reversible lithium-oxygen battery operation for 100 cycles by using lithium perchlorate in dimethyl sulfoxide as the electrolyte and porous gold as the cathode.[6] It has thus become clear that finding the optimum electrode and electrolyte is an important issue in the lithium-oxygen battery field. Most commonly known lithium-oxygen batteries generally use non-aqueous electrolytes, lithium foil as an anode material, and porous carbon as cathode material. The cathode functions as an

oxygen reduction reaction (ORR) and oxygen evolution reaction (OER) catalyst. Since Li_2O_2 generated at discharge determines the capacity of the battery, a cathode material having a large pore volume capable of storing Li_2O_2 is required.[7]

The principle of a lithium-oxygen battery is to generate electricity through a chemical reaction between lithium metal and oxygen. In particular, Li_2O_2 is produced while consuming lithium ions and oxygen at the discharge, and this reaction occurs in the pores of the oxygen cathode. Conversely, during the charging process, the opposite process occurs and oxygen is generated. These chemical reactions are shown below.[8]

$2Li + O_2 = Li_2O_2$, $\Delta G^o = -571.0$ kJ mol^{-1} ($E^o = 2.96$ V)

1.2 Challenges of lithium-oxygen batteries

Despite the superior merit of high theoretical capacity, there are still many problems in commercializing lithium-oxygen batteries. One important obstacle is their low round-trip efficiency (65%) due to parasitic side reactions and instability of the electrolyte.[9-10] These problems are closely linked to the technical barriers that include instability between electrolyte and carbon electrode, kinetic of charging and discharging with slow discharge at the oxygen electrode. The side reaction products are generally insoluble and electrically insulating, gradually blocking the cathode during the battery cycle. Although the clogging of cathodes can be disassembled and removed during charging, the high overpotential required to oxidize them results in low round-trip efficiency. Specifically, considering that the latest lithium-ion battery efficiency is 98% or more, it has a very low efficiency of 65%. And, of course, battery cycle life will also be reduced during the continuous formation and oxidation of side reaction products. As a result, the development of a lithium-oxygen battery as a practical energy storage system (ESS) has a critical technical obstacle due to electrolyte instability. In addition, another problem with lithium-oxygen batteries is their inherent insoluble nature of Li_2O_2 produced during the discharge process. Li_2O_2 blocks the cathode surface, which is a small factor that hinders the extremely high theoretical capacity provided by conventional lithium and oxygen electrochemistry. Furthermore, the mechanism of Li_2O_2 in a particular electrolyte creates a large Li_2O_2 agglomerate at the cathode, which acts as an impediment to charge transfer during charging, resulting in high polarization. To overcome these problems, a lot of researchers have studied soluble catalysts known as redox mediators that facilitate the oxidation of Li_2O_2 during charging.[11-14] However, the chemical instability of these types of materials during battery operation remains an unsolved problem.

1.3 Organic-free electrolyte for high oxygen efficiency

In the case of an organic electrolyte composed of a salt and an organic solvent, since the organic solvent is decomposed at a high potential, researches have been conducted to minimize the use of an organic solvent such as a high concentration organic electrolyte, an ionic liquid, and a solid polymer electrolyte.[15-17] Recently, Addison`s group proposed an innovative approach that does not use a solvent in the electrolyte to solve this fatal issue of organic solvent byproducts. They used a nitrate molten salt as the electrolyte in the lithium-oxygen battery to operate the battery above the eutectic point, resulting in a very low charging potential of 2.85 V, as well as an ideal oxygen evolution during charging.[18]

1.4 A molten salt electrolyte

Studies on molten nitrate salt electrolytes for thermal batteries date back to the 1980s. The reaction between Li metal and nitrate anions has been described as forming a solid-electrolyte interphase (SEI) layer composed of lithium oxide (Li_2O), which is stable enough for primary and secondary cells.[19] Also, Addison`s group predicted that since the electrolyte is operated at high temperature, the solubility of the discharge product (Li_2O_2) can be increased and the kinetic of the electrode will increase as compared to the room temperature organic electrolyte.[18]

Here we attempt to reappear the stable electrolyte for reversible oxygen electrochemical reactions at the cathode using a molten nitrate salt combination such as $LiNO_3$-KNO_3 (eutectic point: 125℃), which has been reported previously. In addition, we will demonstrate the temperature effect of the molten salt electrolyte with lower eutectic points such as Li, Na, K, Ca, Cs-NO_3 (eutectic point: 65℃) mixtures. The following figure 1.1 shows a molten salt electrolyte of five different nitrate salt applied to a lithium-oxygen battery. We used differential electrochemical mass spectrometer (DEMS) instrument capable of pressure monitoring and real-time gas analysis to quantitatively analyze the oxygen electrode process, and x-ray diffraction (XRD) and scanning electron microscopy (SEM) were also performed to observe the discharge products at the oxygen electrode.

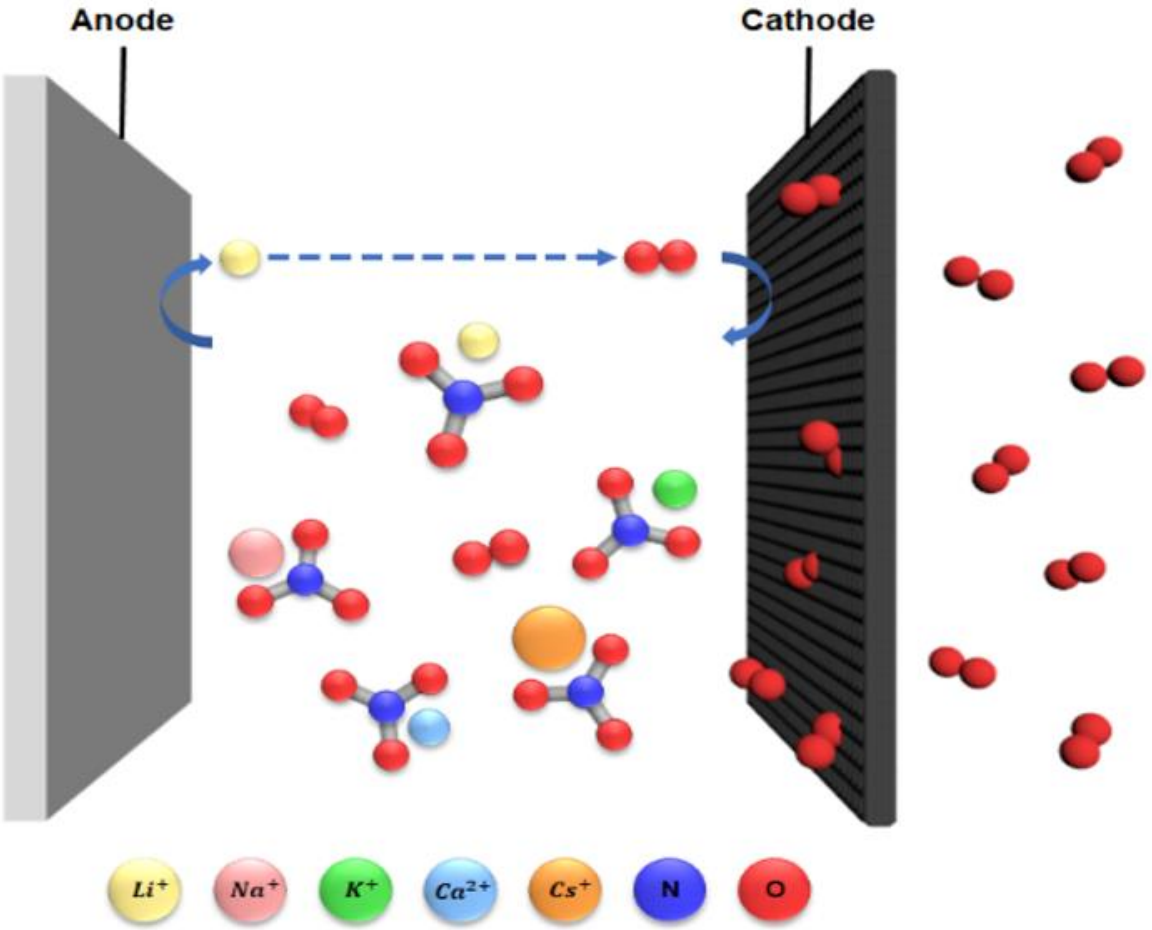

Figure 1.1 five different nitrate molten salts for lithium-oxygen batteries.

1.5 Experimental

1.5.1 Preparation of a molten salt electrolyte and electrode

$LiNO_3$, $NaNO_3$, KNO_3, $CsNO_3$ and $Ca(NO_3)_2$ were purchased from Sigma-Aldrich and kept in a glovebox filled with Ar. The chemical composition and melting point of each electrolyte tested are summarized in the table 2 below.

Table 2. Molten nitrate salt electrolytes used in this work.[18, 20]

Electrolyte	Chemical composition (mol %)	Melting point (℃)
$LiNO_3$-KNO_3	42-58	125
$LiNO_3$-$NaNO_3$-KNO_3-$CsNO_3$-$Ca(NO_3)_2$	15-10-30-30-15	65

Generally, the weight is measured according to the salt composition and then heated with a torch to impregnate the dissolved eutectic mixture with a 16 mm diameter glass fiber separator (GF/C, Whatman) depicted in Figure 1.2.

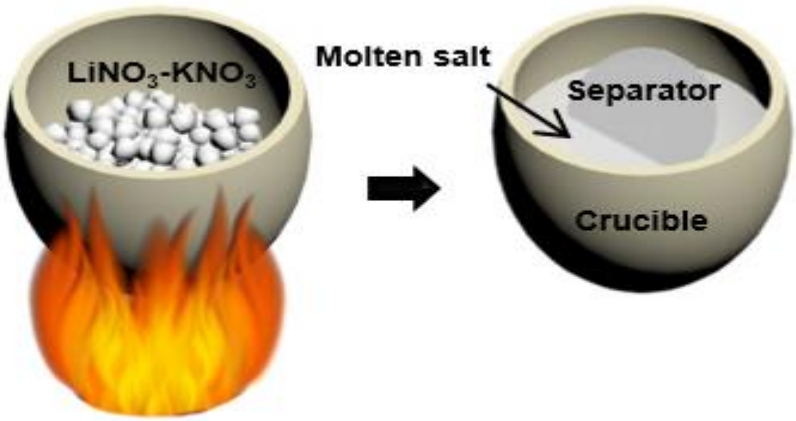

Figure 1.2 Schematic illustrations of a method for a molten salt electrolyte.

The oxygen electrode is made by mixing Super P carbon black (Timcal) and PTFE binder (Sigma-Aldrich) at a mass ratio of 8:2 without catalyst. It is then dried in an oven at 120℃ overnight and then applied to a stainless steel mesh of 12 mm diameter. Typical carbon loading is 2 mg/cm^2 and electrode surface area is 1.1304 cm^2.

1.5.2 Assembly of the lithium-oxygen cell

A coin-type lithium-oxygen laboratory battery consists of lithium metal, Super P cathodes and a glass fiber separator impregnated with a molten salt electrolyte in Figure 1.3. The cell assembly proceeded in a glovebox filled with argon with oxygen and moisture levels of less than 1 ppm. The coin cell is inserted into a cell holder for a lithium-oxygen battery and connected to a pressure sensor and a DEMS instrument capable of quantitative gas analysis. Pure oxygen gas is injected into the battery and leak test is carried out with positive pressure of about 1100 torr each time.

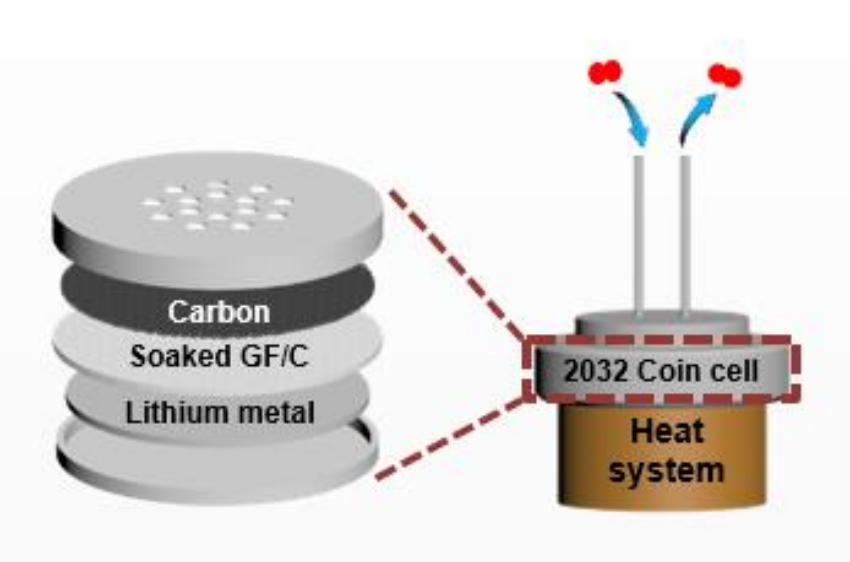

Figure 1.3 2032 coin-type cell structure for lithium-oxygen battery and cell kit for high-temperature operation

1.5.3 Designing cell kit for high-temperature operation

Since the cell is operated above the eutectic point, a cell kit with a high-temperature function was designed by tuning the cell kit at room temperature. As shown in Figure 1.4, we designed so that the battery voltage should be stable in a high-temperature environment and the temperature can be kept constant. Especially, the thermocouple was inserted in the middle to detect the temperature, the cartridge heater on both sides was allowed to heat, and the other side was electrically connected to the 2032 coin cell. The measurement was carried out after waiting until the specific temperature was reached according to the molten salt electrolyte used.

Figure 1.4 cell kit design for high-temperature operation

1.5.4 Oxygen efficiency measurement using differential electrochemical mass spectrometry (DEMS) and electrochemical analysis

Analysis with a DEMS instrument allows pressure monitoring during the discharge to determine the exact amount of oxygen consumed and provides a precise amount of oxygen evolved during charging through the mass spectrometer. Therefore, the oxygen efficiency of the OER/ORR can be obtained through the DEMS instrument shown in Figure 1.5 below. In addition to oxygen, byproduct gases such as carbon dioxide and hydrogen can be measured, and it is possible to know the occurrence of a side reaction in a specific potential, and thus it is utilized as a powerful analysis tool in a lithium-oxygen battery.

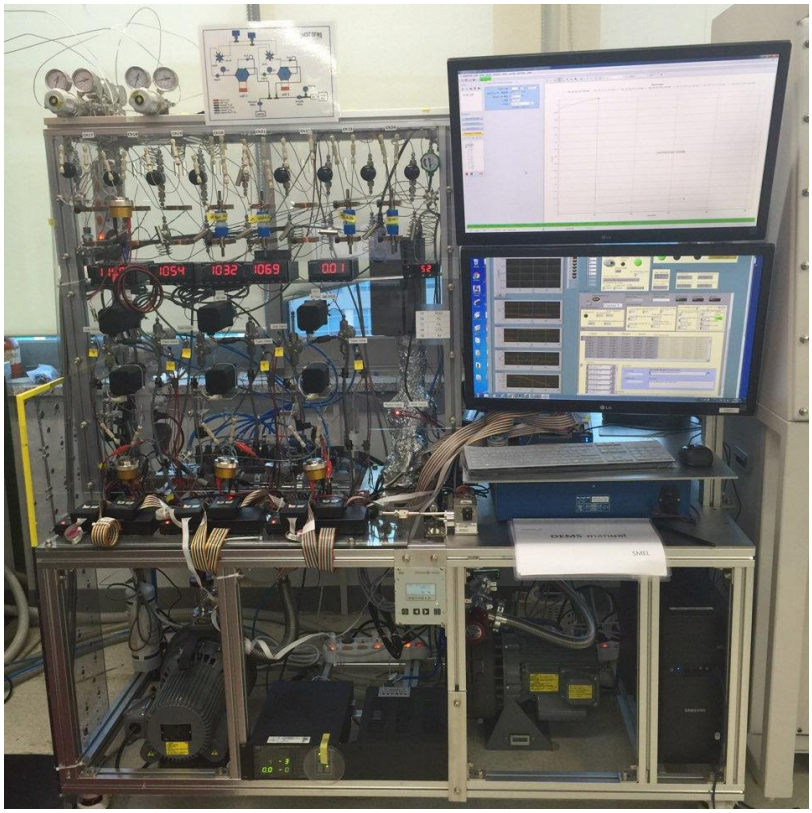

Figure 1.5 Differential Electrochemical Mass Spectrometry (DEMS) instrument for oxygen efficiency measurement of lithium-oxygen batteries.

To evaluate battery performance such as capacity and voltage, galvanostatic cycling at a constant current (200 μA) and linear sweep voltammetry (LSV) analysis were performed simultaneously with the DEMS analysis. The electrochemical performances were measured using a potentio-galvanostat (WonATech, WBCS 3000, Korea). For LSV analysis, the cell potential was linearly swept from OCV to 3.7 V at a scan rate of 0.05 mV/s. Tetraethylene glycol dimethyl ether (TEGDME) and lithium

bis(trifluoromethylsulfonyl) imide (LiTFSI) were purchased from Sigma-Aldrich for the effect of temperature on the organic electrolyte. The electrolyte was prepared by dissolving LiTFSI in TEGDME at a concentration of 1 M and refining the moisture using 4 Å molecular sieves (Sigma-Aldrich). All electrolyte preparation procedures were carried out in a glovebox filled with Ar. A glass fiber (Whatman) with a diameter of 19 mm containing 150 μL of the electrolyte was used in the battery. For the discharge product analysis, the cathode surface was analyzed for each cycle step using XRD (Bruker D8 Advance with Cu Kα from 20 to 70° at a scan rate of 2° min^{-1}). Generally, in the case of the cathode, the cell was disassembled after cooling and the cathode was extracted and washed with NMA solvent to remove the nitrate salt from the residue. The electrode was then sealed with a Kapton tape to prevent exposure to air. SEM analysis was performed using a Hitachi High-Technologies, S-4800 instrument and electrode preparation similar to XRD was rinsed with NMA solvent before entering the analyzer.

1.6 Result and Discussion

Figure 1.6.a shows a SEM image and an optical photograph (inset) of a glass fiber separator containing a molten salt electrolyte of $LiNO_3$-KNO_3. Figure 1.6.b shows a detailed phase diagram showing the eutectic point behavior of molten salts. The coin type cell inserted in figure 1.b shows before (two solid phase) and after (one liquid phase) the eutectic point.

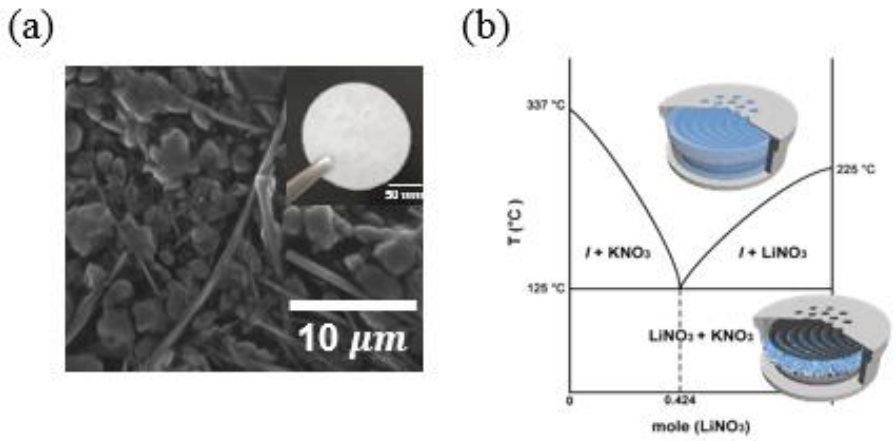

Figure 1.6 (a) SEM image of the prepared a molten salt electrolyte ($LiNO_3$-KNO_3) and inset is an optical photograph, (b) Phase diagram of binary mixture.

The performance of a molten salt electrolyte was examined using a coin-type cell composed of a lithium metal anode, molten salt electrolyte ($LiNO_3$-KNO_3) impregnated into a glass fiber separator at 150℃, and a porous Super P cathode. The cell was run with a capacity (1 mAh) after fully discharging to avoid side reactions. Figure 1.7.a is the voltage profile of discharging and charging at 200 μA constant current as a result of reappearing previously reported data. It is confirmed that the binary molten salt shows very low voltage gap (~0.1 V) in agreement with the results of the previous paper.[18] Figure 1.7.b shows the results of the in situ gas analysis, in which the oxygen gas increases at the beginning of the charge and remains constant during the entire charge cycle. It also showed that no other gases such as carbon dioxide and nitric oxide were produced.

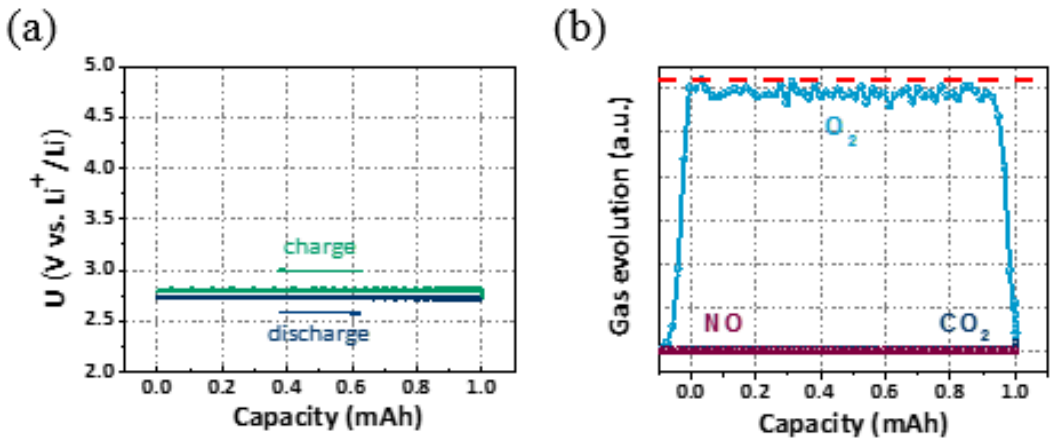

Figure 1.7 (a) Galvanostatic discharge-charge profile to a 1 mAh cut off, (b) in situ gas analysis for lithium-oxygen battery during charging, applying a current of 200 μA and fixed capacity regime of 1 mAh.

Figure 1.8 shows the result of gas evolution analysis while charging from OCV to 3.7 V at a scan rate of 0.05 mV/s using LSV-DEMS analysis. Oxygen evolution reaction occurs from 2.8 V to 3.0 V, with a maximum of 2.9 V. Other gases such as carbon dioxide and nitric oxide are monitored in the 3.3-3.7 V range. These would arise from oxidation reactions of the carbon electrode material and the electrolyte materials, NO_3^-.

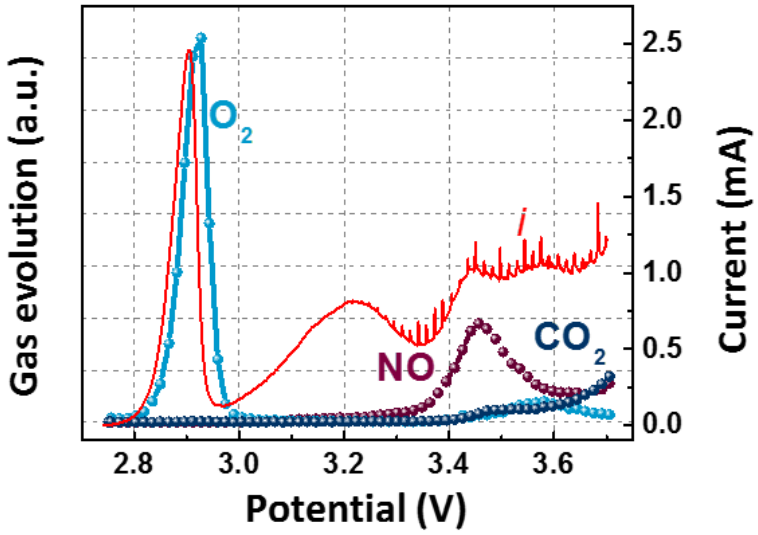

Figure 1.8 LSV-DEMS analysis of gas evolution with charging at a scan rate of 0.05 mV/s.

Previously, the binary mixture electrolyte was successfully reproduced and then $LiNO_3$-$NaNO_3$-KNO_3-$CsNO_3$-$Ca(NO_3)_2$ the eutectic mixture having a lower eutectic point was found and operated at 100℃. The quinary mixture of nitrate salts has a lower melting point (65℃) than the binary mixture, enabling it to operate at lower temperatures. Figure 1.9 shows a photograph at 100℃ of the left vial showing a solid phase with five different salts and a right vial showing the molten salt in one liquid phase after passing through the melting point.

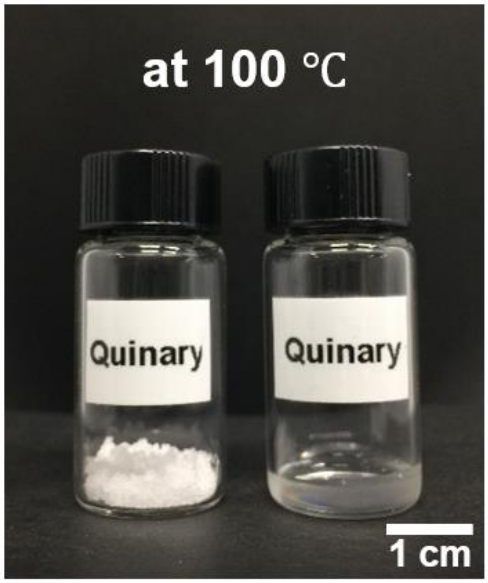

Figure 1.9 Photograph at 100℃ of the prepared quinary mixture before and after passing melting points.

Figure 1. 10 shows the temperature-dependent voltage profile of a lithium-oxygen battery using quinary molten salt electrolyte and oxygen evolution during charging. As the temperature increases, the overpotential of the cell decreases (especially the charging voltage is greatly reduced) and the oxygen evolution reaction increases. For example, figure 1.10.a, c and e show that as the temperature gradually increases from 100℃ to 120℃ to 150℃, the maximum charge voltage gradually decreases from 3.84 V to 3.44 V to 2.93 V. These temperature-related trends were also associated with DEMS results, which indicate oxygen evolution efficiency during charging. As the temperature increased, the OER/ORR ratio also increased to 51%, 65%, and 90%. This is because not only the mobility of oxygen in the electrolyte is increased, but also the viscosity of the electrolyte is decreased, and the resistance required for decomposition of Li_2O_2, the discharge product is reduced by increasing the solubility of Li_2O_2.

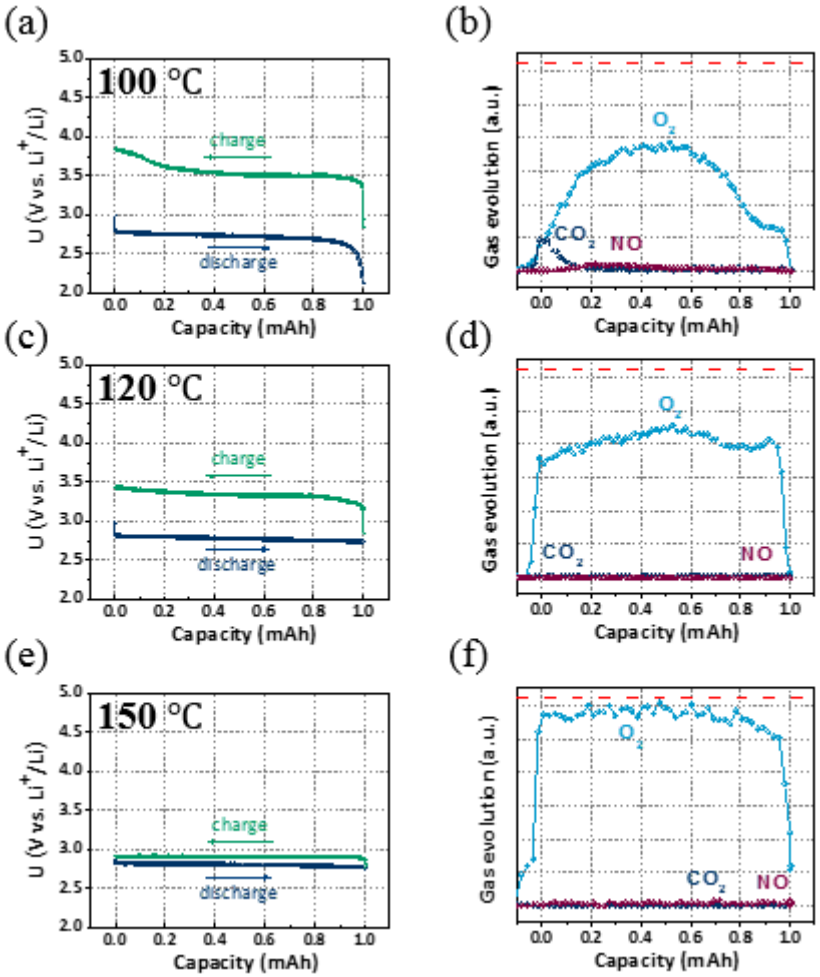

Figure 1.10 Galvanostatic discharge-charge voltage profile using a quinary molten salt electrolyte with in situ DEMS analysis for lithium-oxygen battery during charging, applying a current of 200 μA and a fixed capacity regime of 1 mAh (a,b) at 100℃. (c,d) at 120℃. (e,f) at 150℃ (the dotted line in b, d, f indicates the ideal 2 e^-/O_2 process).

For the characterization of discharge products, the oxygen side of the cathode was analyzed by XRD and SEM after fully discharging in an oxygen atmosphere (Figure 1. 11). The XRD results clearly show that crystalline Li_2O_2 is clearly formed on the surface of the cathode after discharge, depending on the temperature. SEM analysis was also carried out to investigate the morphology of the discharge products at the oxygen electrode. In general, particles with a size of less than 20 microns were observed on the cathode surface and the morphology of Li_2O_2 was hexagonal. The hexagonal form is known to be the most stable morphology of Li_2O_2.[21-22] Figure 1.11.b is a SEM image of a quinary molten salt comparing the surface of a completely discharged carbon cathode under oxygen with temperature. As the temperature increases, the size of the discharge product, Li_2O_2, decreases. The carbon electrode was prepared by rinsing with NMA solvent to remove residual nitrate salt.

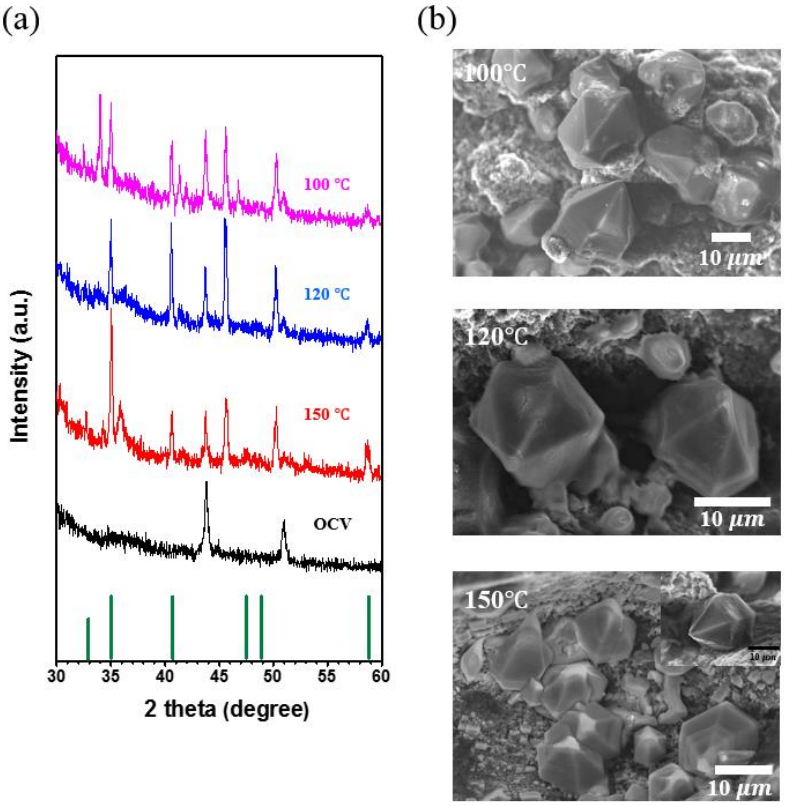

Figure 1. 11 (a) XRD and (b) SEM analysis of a Super P carbon electrode after a full discharge in quinary molten salt electrolyte at 100, 120, 150℃.

To further investigate the effect of temperature on charging overpotentials in a lithium-oxygen cell, the temperature-dependent LSV-DEMS analysis was performed in Figure 1. 12. It clearly shows that the anodic current appears at the lower potential as temperature increases. This is because the solubility of Li_2O_2 as an intermediate and Li_2O_2 as a discharge product increases with increasing temperature. At 150℃, the kinetic of the electrode would increase and the ionic conductivity of the molten salt electrolyte would increase and the internal cell resistance would have decreased. The higher the temperature, the more the anodic peak moves to the left and the oxygen generating peaks move accordingly. In all cases, the decomposition of the molten salt electrolyte results in the generation of nitric oxide gas from 3.4 V. And decomposition of carbon becomes evident above 3.6 V.

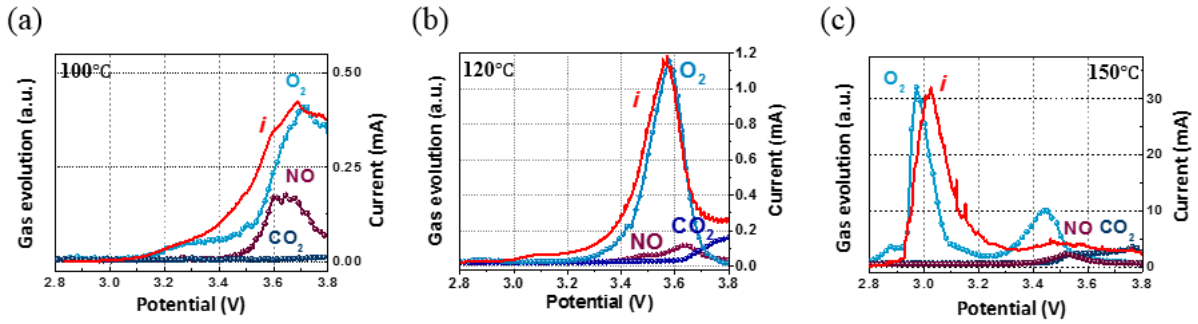

Figure 1. 12 LSV-DEMS analysis showing oxygen, nitric oxide, carbon dioxide gas evolution and anodic peak from 2.8 V to 3.8 V at a scan rate of 0.05 mV/s (a) at 100 ℃, (b) at 120 ℃, (c) at 150 ℃.

Figure 1. 13 shows ORR discharge graphs and power measurement of a lithium-oxygen cell at different temperatures. This graph was obtained by sweeping the current from 0 mA to -24 mA at a scan rate of -0.05 mA s^{-1} and discharging at a cut-off condition of 0.2 V. The maximum power value increases nearly 18 times from 0.76 mW to 13.67 mW when the operating temperature is increased from 100 to 150℃.

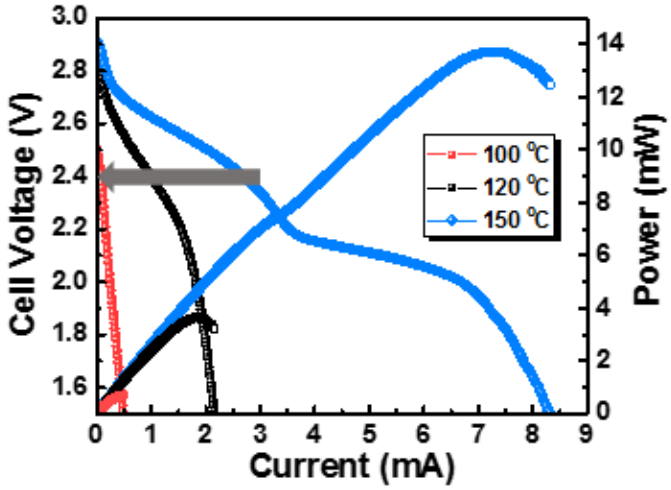

Figure 1. 13 Effect of temperature on power performance of lithium-oxygen cell.

The rate capability experiment was also performed at 150℃. The discharge and charge voltage profiles for different currents at 150℃ are shown in Figure 1. 14. As the current increases, the overpotential increases slightly. This demonstrates that using molten salt electrolytes at high temperatures, the battery conversion efficiency is high even under harsh conditions such as high current.

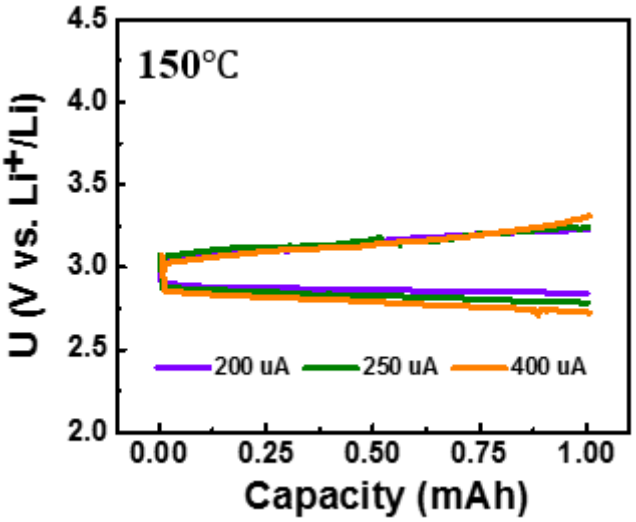

Figure 1. 14 Discharge and charge voltage profile of lithium-oxygen cell at different current at 150℃.

As the temperature increases, the viscosity of the electrolyte decreases, which leads to the effect of facilitating the movement of oxygen and lithium ions. We have observed the positive effect of temperature on the molten salt electrolyte in terms of voltage gap and power.

1.7 Conclusion

We found that by replacing volatile and unstable organic electrolytes with inorganic electrolytes, they are chemically very stable in lithium-oxygen batteries. We have reproduced that the experiment using the binary mixture electrolyte, a previously reported alkali nitrate salt, and studied the oxygen electrochemical reaction with the temperature effect using a quinary mixture with a lower melting point. Oxygen reduction reaction revealed that it was a 2 e^-/O_2 reaction. The XRD confirmed that the most stable Li_2O_2 form, hexagonal shape, and the ORR kinetic at higher temperature were further increased. The oxygen evolution reaction proceeded by gas analysis and observed not only the ideal oxygen evolution but also the decomposition of the electrolyte at 3.4 V by the LSV-DEMS analysis.

Chapter 2

2. Organic-free electrolyte for rechargeable lithium-carbon dioxide batteries

2.1 Introduction of rechargeable lithium-carbon dioxide batteries

Over the past decade, metal-air batteries have received huge worldwide attention, but technical limitations remain a problem. It has a very large energy density because it can be used as oxygen electrode rather than storing the active cathode material in a battery. Lithium-oxygen battery, which uses pure oxygen, has a disadvantage in that it has many limitations to replace atmospheric air and is vulnerable to water and carbon dioxide.[23] Carbon dioxide is present in very low concentrations in the atmosphere, but it has excellent solubility in organic solvents, 50 times better than oxygen, and is highly reactive.[24] Interestingly, recently, a study on lithium-carbon dioxide using CO_2 itself as a reaction gas has emerged as an eco-friendly battery capable of mitigating a large amount of CO_2 emissions. This battery has been known to be based on the reaction of $4Li + 3CO_2 \leftrightarrow 2Li_2CO_3 + C$.[25-27] The concept of a Li-CO_2 primary battery using an ionic liquid at high temperature was first introduced by the Archer group and then the rechargeable Li-CO_2 secondary battery was developed by applying a liquid organic electrolyte.[25, 28] However, Li_2CO_3, which is discharge product of Li-CO_2 battery compared to amorphous porous Li_2O_2, which is a discharge product of Li-O_2 battery, is a thick, polymer-like shape without pores. This limits the electrochemical performance and causes a large polarization. To solve this problem, the reversible Li-CO_2 battery with high discharge capacity (8829 mAh g^{-1}) and high coulombic efficiency of 86.2 % in the first cycle was obtained by using ruthenium, which has excellent catalytic activity in the Zhou group, as the cathode catalyst of the Li-CO_2 battery.[29]

In this work, we report on the application of organic electrolytes and inorganic electrolytes for Li-CO_2 batteries. Especially, the decomposition reaction of Li_2CO_3 was analyzed by in situ gas analysis.

2.2 Experimental

Here, we have constructed a Li-CO_2 battery consisting of a lithium foil anode and an organic-free binary molten salt ($LiNO_3$-KNO_3) electrolyte and a Super P cathode. For the organic electrolyte, 1 M LiTFSI in TEGDME was used. The same as the above-mentioned experimental method in Chapter 1, but the only difference is that the reactant gas is changed by injecting carbon dioxide gas instead of oxygen gas. The assembled Li-CO_2 battery is operated into a coin-type cell at a fixed capacity of 1 mAh. This study shows the basic research process of the Li-CO_2 battery. The configuration of the Li-CO_2 battery using molten salt electrolytes is depicted in Figure 2.1. In addition, in order to understand the electrochemical oxidation of Li_2CO_3, an electrode filled with Li_2CO_3 and a conductive carbon material showing a discharged state was used.[30] A DEMS instrument was used to analyze the gas generated during charging with this pre-filled electrode, and XRD was used to analyze the components of the electrode.

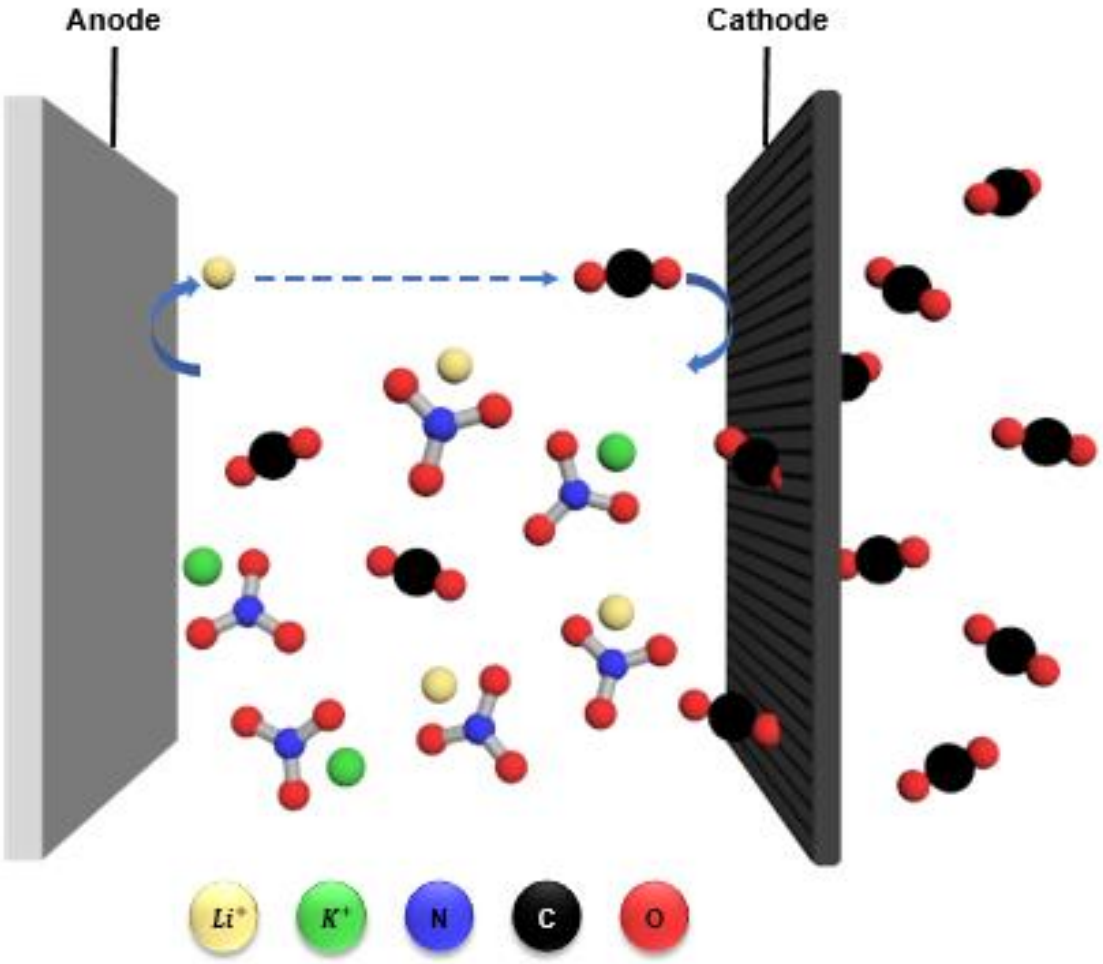

Figure 2.1 lithium and potassium nitrate molten salts for lithium-carbon dioxygen batteries.

2.3 Result and discussion

Figure 2.2 shows the result of applying a general organic electrolyte, 1 M LiTFSI in TEGDME and Ketjen black (KB) electrode. The charging voltage of the inorganic (molten salt, $LiNO_3$-KNO_3) electrolyte was 3.2 V, which was lower than the charging voltage of organic electrolyte of 4.5 V, but the inorganic electrolyte did not generate carbon dioxide. Studies on gaseous charged products and electrolytes should be further investigated.

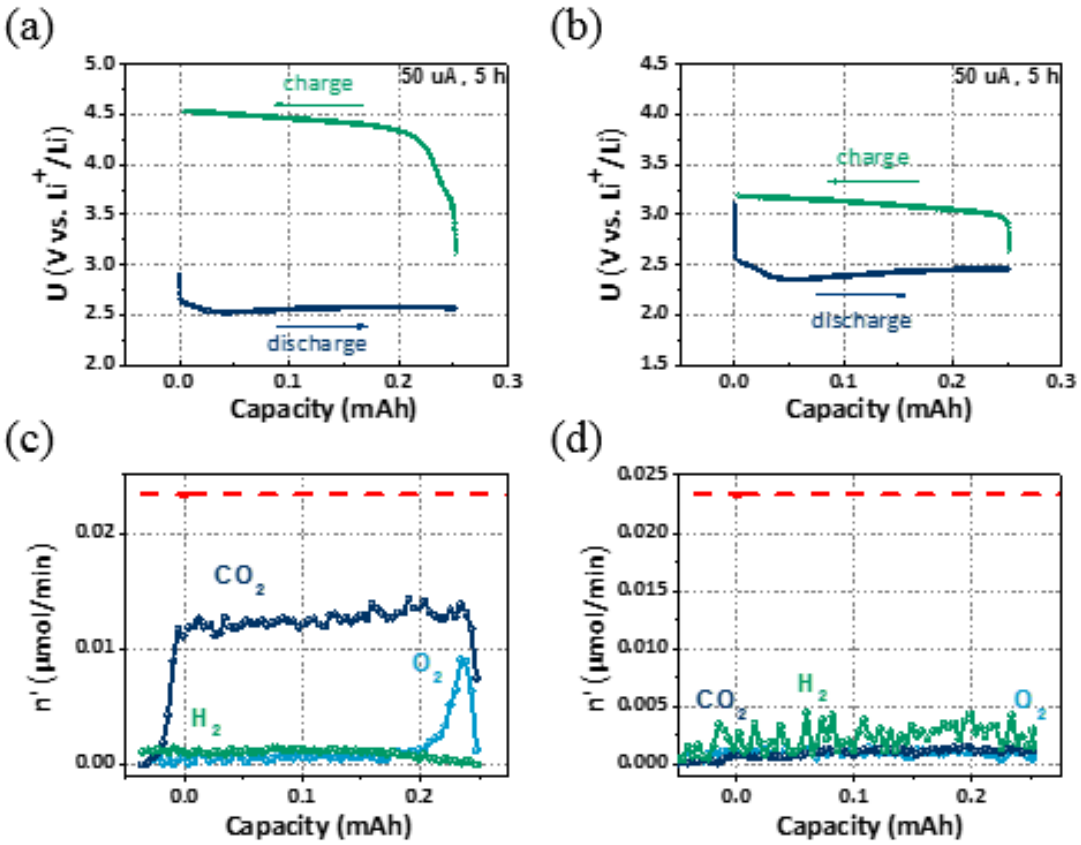

Figure 2.2 The first discharge/charge profiles with 1 M LiTFSI in TEGDME electrolyte (a) and molten salts electrolyte, $LiNO_3$-KNO_3 (b). Gas evolution profile during charge process of Li-CO_2 cell with limited capacity of 0.25 mAh obtained using in-situ DEMS anlaysis using organic electrolyte (c) and inorganic electrolyte (d).

XRD analysis of the Li-CO_2 cell shown in Figure 2.3 demonstrates that the discharge product, Li_2CO_3, is more evident in the inorganic electrolyte ($LiNO_3$-KNO_3 molten salt) after discharge. The research on the discharge products according to the electrolyte should be further proceeded.

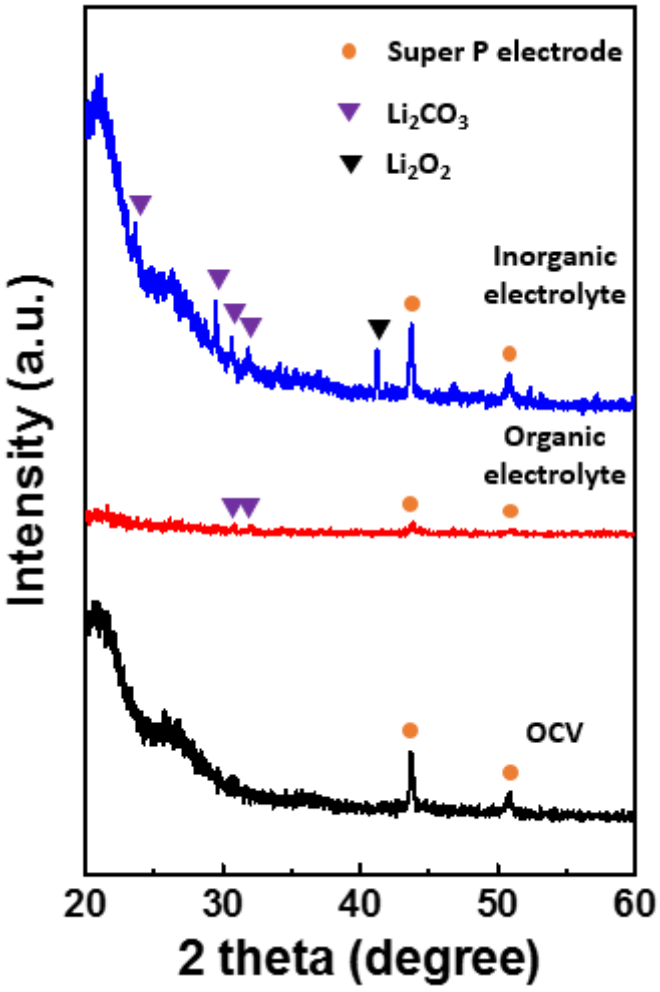

Figure 2.3 XRD analysis of the cathode in Li-CO_2 battery following an OCV (before discharge), a discharge in organic electrolyte (1 M LiTFSI in TEGDME), and a discharge in inorganic electrolyte ($LiNO_3$-KNO_3 molten salt) at 150℃.

Figure 2.4 shows the charge profile of the electrode pre-filled with conductive carbon material and Li_2CO_3 when organic and inorganic electrolytes were used. As shown in Figure 2.2, only Li_2CO_3 was decomposed in the organic electrolyte, but no gas was produced in the inorganic electrolyte.

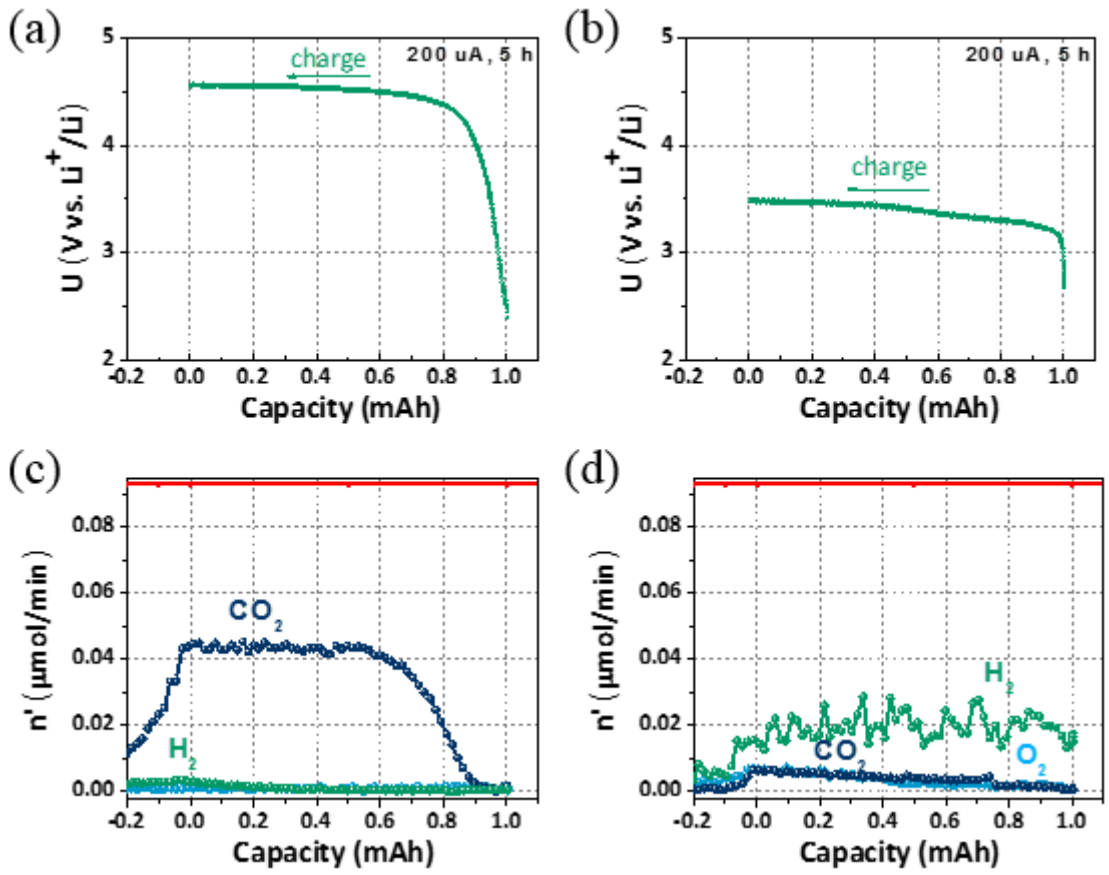

Figure 2.4 Charge profile and gas evolution profile during charging of the cathode electrode pre-filled by Li_2CO_3 with KB as conductive additive under argon atmosphere with Li foil as anode. (a,c) 1 M LiTFSI in TEGDME was used as organic electrolyte. (b,d) $LiNO_3$-KNO_3 molten salt was used as inorganic electrolyte.

When an organic electrolyte and an inorganic electrolyte are used, a conductive carbon material and Iridium having an excellent catalytic activity for Li_2CO_3 are added to the electrode, and the charging profile of the electrode is shown in Figure 2.4. It was found that the charging voltage slightly reduced when the Ir catalyst was used and the decomposition efficiency of Li_2CO_3 was increased in the case of the organic electrolyte. However, it was confirmed that Li_2CO_3 was decomposed and not released into CO_2 even in the case of molten salt electrolyte when using Ir catalyst.

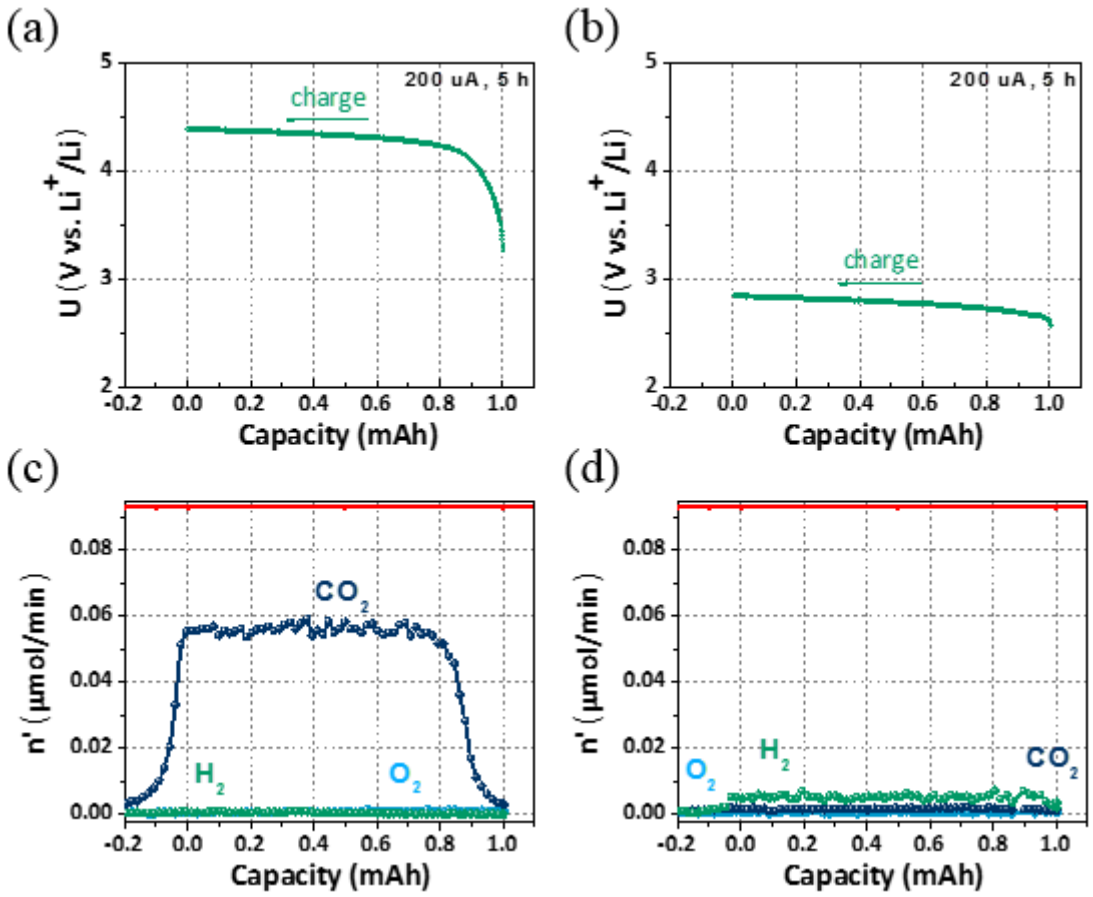

Figure 2.5 Charge profile and gas evolution profile during charging of the cathode electrode pre-filled by Li_2CO_3 and KB with Ir as catalyst for Li_2CO_3 decomposition under argon atmosphere with Li foil as anode. (a.c) 1 M LiTFSI in TEGDME was used as organic electrolyte. (b,d) $LiNO_3$-KNO_3 molten salt was used as inorganic electrolyte.

2.4 Conclusions

In summary, we investigated the electrochemical reactions of Li_2CO_3 formation and oxidation using organic electrolytes and inorganic electrolytes. XRD analysis also confirmed that Li_2CO_3 were major discharge products. Additionally, DEMS analysis confirmed that CO_2 was detected as the main gas product the charging process using Li_2CO_3 electrode. In the case of organic electrolytes, the excellent catalytic activity of Ir@KB lowers the charging voltage and increases the amount of CO_2 generated.

References

1. Tarascon, J.-M.; Armand, M., Issues and challenges facing rechargeable lithium batteries. *Nature* **2001,** *414* (6861), 359-367.
2. Bruce, P. G.; Freunberger, S. A.; Hardwick, L. J.; Tarascon, J.-M., Li-O2 and Li-S batteries with high energy storage. *Nature materials* **2012,** *11* (1), 19-29.
3. Li, F.; Zhang, T.; Zhou, H., Challenges of non-aqueous Li–O 2 batteries: electrolytes, catalysts, and anodes. *Energy & environmental science* **2013,** *6* (4), 1125-1141.
4. Abraham, K.; Jiang, Z., A polymer electrolyte-based rechargeable lithium/oxygen battery. *Journal of The Electrochemical Society* **1996,** *143* (1), 1-5.
5. Ogasawara, T.; Débart, A.; Holzapfel, M.; Novák, P.; Bruce, P. G., Rechargeable Li2O2 electrode for lithium batteries. *Journal of the American Chemical Society* **2006,** *128* (4), 1390-1393.
6. Peng, Z.; Freunberger, S. A.; Chen, Y.; Bruce, P. G., A reversible and higher-rate Li-O2 battery. *Science* **2012,** *337* (6094), 563-566.
7. McCloskey, B. D.; Scheffler, R.; Speidel, A.; Bethune, D. S.; Shelby, R. M.; Luntz, A., On the efficacy of electrocatalysis in nonaqueous Li–O2 batteries. *Journal of the American Chemical Society* **2011,** *133* (45), 18038-18041.
8. Chase Jr, M., NIST–JANAF thermochemical tables, 4th edn, Part II, Cr–Zr. *J. Phys. Chem. reference data, Monograph* **1998,** (9).
9. Luntz, A. C.; McCloskey, B. D., Nonaqueous Li–air batteries: a status report. *Chemical reviews* **2014,** *114* (23), 11721-11750.
10. Freunberger, S. A.; Chen, Y.; Drewett, N. E.; Hardwick, L. J.; Bardé, F.; Bruce, P. G., The lithium–oxygen battery with ether-based electrolytes. *Angewandte Chemie International Edition* **2011,** *50* (37), 8609-8613.
11. Chen, Y.; Freunberger, S. A.; Peng, Z.; Fontaine, O.; Bruce, P. G., Charging a Li–O2 battery using a redox mediator. *Nature chemistry* **2013,** *5* (6), 489-494.
12. Chase, G. V.; Zecevic, S.; Wesley, T. W.; Uddin, J.; Sasaki, K. A.; Vincent, P. G.; Bryantsev, V.; Blanco, M.; Addison, D. D., Soluble oxygen evolving catalysts for rechargeable metal-air batteries. Google Patents: 2011.
13. Lim, H.-D.; Lee, B.; Zheng, Y.; Hong, J.; Kim, J.; Gwon, H.; Ko, Y.; Lee, M.; Cho, K.; Kang, K., Rational design of redox mediators for advanced Li–O2 batteries. *Nature Energy* **2016,** *1*, 16066.
14. Kundu, D.; Black, R.; Adams, B.; Nazar, L. F., A highly active low voltage redox mediator for enhanced rechargeability of lithium–oxygen batteries. *ACS central science* **2015,** *1* (9), 510-515.
15. Giordani, V.; Uddin, J.; Bryantsev, V. S.; Chase, G. V.; Addison, D., High Concentration Lithium Nitrate/Dimethylacetamide Electrolytes for Lithium/Oxygen Cells. *Journal of The Electrochemical Society* **2016,** *163* (13), A2673-A2678.
16. Elia, G.; Hassoun, J.; Kwak, W.-J.; Sun, Y.-K.; Scrosati, B.; Mueller, F.; Bresser, D.; Passerini, S.; Oberhumer, P.; Tsiouvaras, N., An advanced lithium–air battery exploiting an ionic liquid-based electrolyte. *Nano letters* **2014,** *14* (11), 6572-6577.

17. Balaish, M.; Peled, E.; Golodnitsky, D.; Ein-Eli, Y., Liquid-Free Lithium–Oxygen Batteries. *Angewandte Chemie International Edition* **2015,** *54* (2), 436-440.

18. Giordani, V.; Tozier, D.; Tan, H.; Burke, C. M.; Gallant, B. M.; Uddin, J.; Greer, J. R.; McCloskey, B. D.; Chase, G. V.; Addison, D., A molten salt lithium–oxygen battery. *Journal of the American Chemical Society* **2016,** *138* (8), 2656-2663.

19. Miles, M.; Fletcher, A., Cation effects on the electrode reduction of molten nitrates. *Journal of The Electrochemical Society* **1980,** *127* (8), 1761-1766.

20. Raade, J. W.; Padowitz, D., Development of molten salt heat transfer fluid with low melting point and high thermal stability. *Journal of Solar Energy Engineering* **2011,** *133* (3), 031013.

21. Radin, M. D.; Rodriguez, J. F.; Tian, F.; Siegel, D. J., Lithium peroxide surfaces are metallic, while lithium oxide surfaces are not. *Journal of the American Chemical Society* **2011,** *134* (2), 1093-1103.

22. Mo, Y.; Ong, S. P.; Ceder, G., First-principles study of the oxygen evolution reaction of lithium peroxide in the lithium-air battery. *Physical Review B* **2011,** *84* (20), 205446.

23. Christensen, J.; Albertus, P.; Sanchez-Carrera, R. S.; Lohmann, T.; Kozinsky, B.; Liedtke, R.; Ahmed, J.; Kojic, A., A critical review of Li/air batteries. *Journal of the Electrochemical Society* **2011,** *159* (2), R1-R30.

24. Wadhawan, J. D.; Welford, P. J.; Maisonhaute, E.; Climent, V.; Lawrence, N. S.; Compton, R. G.; McPeak, H. B.; Hahn, C. E., Microelectrode studies of the reaction of superoxide with carbon dioxide in dimethyl sulfoxide. *The Journal of Physical Chemistry B* **2001,** *105* (43), 10659-10668.

25. Xu, S.; Das, S. K.; Archer, L. A., The Li–CO 2 battery: A novel method for CO 2 capture and utilization. *RSC Advances* **2013,** *3* (18), 6656-6660.

26. Takechi, K.; Shiga, T.; Asaoka, T., A Li–O 2/CO 2 battery. *Chemical Communications* **2011,** *47* (12), 3463-3465.

27. Xie, Z.; Zhang, X.; Zhang, Z.; Zhou, Z., Metal–CO2 Batteries on the Road: CO2 from Contamination Gas to Energy Source. *Advanced Materials* **2017,** *29* (15).

28. Liu, Y.; Wang, R.; Lyu, Y.; Li, H.; Chen, L., Rechargeable Li/CO 2–O 2 (2: 1) battery and Li/CO 2 battery. *Energy & Environmental Science* **2014,** *7* (2), 677-681.

29. Yang, S.; Qiao, Y.; He, P.; Liu, Y.; Cheng, Z.; Zhu, J.-j.; Zhou, H., A reversible lithium–CO 2 battery with Ru nanoparticles as a cathode catalyst. *Energy & Environmental Science* **2017,** *10* (4), 972-978.

30. Yang, S.; He, P.; Zhou, H., Exploring the electrochemical reaction mechanism of carbonate oxidation in Li–air/CO 2 battery through tracing missing oxygen. *Energy & Environmental Science* **2016,** *9* (5), 1650-1654.